The Application of Drop Size Distribution and Discrete Drop Mass Transfer Models to Assess the Performance of a Rotating Disc Contactor

A method has been developed to calculate the overall mass transfer coefficient in an agitated liquid extraction column containing a wide range of drop sizes. The method applied the drop size distribution diagram to estimate the volume percentage of stagnant, circulating, and oscillating drops in the drop population. Individual mass transfer coefficients were then evaluated for the corresponding drop state, using the different single-drop mass transfer models, after which the overall coefficient K_{cal} was calculated as the fractional sum of the individual coefficients and their proportion in the drop population. These estimated mass transfer coefficients have been compared with results obtained from a large rotating disc extractor 0.45 m in diameter and 6.75 m high, extracting acetone between water and Clairsol (a parafinic hydrocarbon, principally decane). Good agreement was obtained in the majority of the experiments when the Rose-Kintner correlation was applied to evaluate the dispersed phase mass transfer coefficient of the oscillating drops. In all experiments agreement between the calculated and experimental overall mass transfer coefficients was improved by evaluating the concentration driving force by applying Simpson's rule, thereby introducing corrections for the variation in flowrate along the column and for possible backmixing.

K. K. AL-ASWAD,
C. J. MUMFORD and
G. V. JEFFREYS

Department of Chemical Engineering
University of Aston in Birmingham
Birmingham B4 7ET, England

SCOPE

In all liquid extraction equipment the dispersed phase exists in the form of drops. In order to analyze the performance of this type of equipment the assumption is made that these drops are spherical and of uniform size. This simplifies the application of discrete drop models of mass transfer to the assessment of equipment performance. Olney (1964) pointed out that such an assumption would lead to serious error, since a distribution of drop sizes always exists in each compartment, or column section, in all extraction equipment. In most mechanically agitated extraction contactors the drop size distribution is the result of competing effects, namely, the generation of new drops through breakup by shear or local turbulence in the bulk flow, and the coalescence due to interactions between the drops. This size distribution is bounded by an upper limit or maximum drop size (Mugele and Evans, 1951) and a lower limit, or minimum drop size, dependent upon the prevailing breakup processes (Olney, 1964). Mass transfer during drop passage through the continuous phase is significantly affected by these hydrodynamic effects, i.e., whether the liquid inside the drops is stagnant, circulating, or oscillating. This has a pronounced effect on the mechanism and therefore rate of mass transfer. The dispersion in an agitated contactor may contain all these types of drops in significant quantities and they must be included in the analysis of the performance of this type of equipment, otherwise reasonable comparison with practical results cannot be expected.

At present the correlations of mass transfer rate and mass transfer coefficient are based on single-drop models; the effects of the presence of adjacent drops have not been assessed hitherto. Droplet collison will certainly induce temporary oscillation in nonoscillating drops but the rate at which these are damped out is not known. Therefore, the introduction of a drop size distribution with the consequences of applying the different discrete drop models is a worthwhile investigation and constitutes the scope of this paper.

CONCLUSIONS AND SIGNIFICANCE

The analysis of the performance of a mechanically agitated column has been undertaken when it was shown that flow variations and backmixing effects can be allowed for by analyses of the extract and raffinate concentrations along the length of the column and thereafter applying Simpson's rule to obtain the mean driving force. In addition, the drop size distribution in the equipment can be described by the Mugele-Evans upper limit law, inferring that mass transfer occurs simultaneously by different mechanisms in different drops depending on drop size. The application of the different discrete drop models, in proportion to the fraction of the

stagnant, circulating, and oscillating drops present in the swarm in the equipment demonstrated that reasonably good agreement between the experimental and calculated coefficients was obtained when the Rose-Kintner oscillating drop model was applied to the portion of the drops which were oscillating. Furthermore it appears that at the holdup levels employed in this study the effects of adjacent drops had no significant effect upon the mass transfer rate.

INTRODUCTION

In all liquid extraction processes one phase is dispersed in the other in the form of drops having a wide distribution of drop sizes. The result is that stagnant, circulating, and oscillating drops coexist in the dispersion and each type of drop therein will be associated with a particular mass transfer mechanism. Therefore the mass transfer rate and coefficients found in practice will differ considerably from those obtained theoretically by applying a specific single-drop model of mass transfer based upon the mean drop size and conditions prevailing in the equipment. In practice, the different mass transfer mechanisms pertaining to the different drop types will occur simultaneously in the swarm of drops in the equipment. The result is that the mass transfer rate for the equipment as a whole will be a composite rate, embracing all the mass transfer processes occurring between the different types of drops and the continuous phase in proportion to the drop size distribution existing in the drop population.

The most reliable single-drop models for estimating the dispersed and continuous phase mass transfer coefficients are summarized in Eqs. 1–7 in Table 1. There it will be seen that the mass transfer coefficient of each phase is greatly affected by the fluid conditions inside the drop, as characterized by the drop Reynolds number. Since the physical properties and hydrodynamic conditions will be the same for all the drops in the fluid regime, the mode of mass transfer will be dependent on drop size. Hence, it is necessary to ascertain the drop size and size distribution in the dispersion passing through the equipment in order to assess its mass transfer performance. Typical drop size distributions on a cumulative volume percent basis are shown in Figure 1. There it will be seen that the stagnant drop regime is characterized by a maximum Reynolds number of 10 and the circulating drop regime by a maximum Reynolds number of 200, and that oscillating drops exist in the system when their Reynolds number exceeds 200. In the evaluation of the drop Reynolds number the drop velocity is taken to be the slip velocity which will be characteristic of the type of extraction column employed, the flowrates of the continuous and dispersed phases, and the dispersed phase holdup in the equipment. Once the maximum drop size for each fluid regime has been estimated, the mean drop size can be ascertained and the mean overall mass transfer coefficient for the particular fluid regime calculated from the single-drop correlations presented in Table 1. Thereafter the mean overall mass transfer coefficient for the equipment can be estimated from the drop size distribution diagram, as the fractional sum of the individual overall coefficients of each regime in proportion to the volume fraction of that regime in the drop population in the equipment. Thus the calculated overall mass transfer coefficient for the extraction column K_{cal} will be:

$$K_{cal} = K_s p_s + K_c p_c + K_o p_o \tag{8}$$

where p_s, p_c, and p_o are the volume fractions of drops in the stagnant, circulating, and oscillating drop regimes, respectively, and K_s, K_c, and K_o are the overall mass transfer coefficients pertaining to each regime.

The proportion of the drop population was based on the volume fraction, rather than say the area fraction, because the mass transfer coefficient of an oscillating drop is of the order of five times greater than that of a circulating drop; therefore the solute concentration in the oscillating drops will become considerably greater than that

TABLE 1. MASS TRANSFER COEFFICIENT MODELS

State of Droplet	Reynolds Number	Dispersed Phase Coefficient Model	Eq. No.	Continuous Phase Coefficient Model	Eq. No.
Stagnant	$Re < 10$	$k_{d.s} = \frac{4\pi^2 D_d}{3d_s}$	(1)	$Sh_{c.s} = 2.076\,(Re)^{0.5}\,(Sc)^{0.3}$	(2)
		Treybal (1963)		Rowe (1965)	
Circulating	$10 < Re < 200$	$k_{d.c} = \frac{17.9 D_d}{d_c}$	(3)	$Sh_{c.c} = -126 + 1.8\,(Re)^{0.5}(Sc)^{0.42}$	(4)
Oscillating	$Re > 200$	Kronig and Brink (1960) $k_{d.o} = 0.45\,(\omega D_d)^{0.5}$ Rose Kintner (1966)	(5)	Garner-Foord Tayeban (1959) $Sc_{c.o} = 50 + 0.0085\,(Re)\,(Sc)^{0.7}$	(7)
		$k_{d.o} = \sqrt{\frac{4\omega D_d(1+\epsilon_o)}{\pi}}$	(6)	Garner-Tayeban (1960)	
		where $\epsilon_o = \epsilon + \frac{3}{8}\epsilon^2$ Angelo-Lightfoot (1966)			

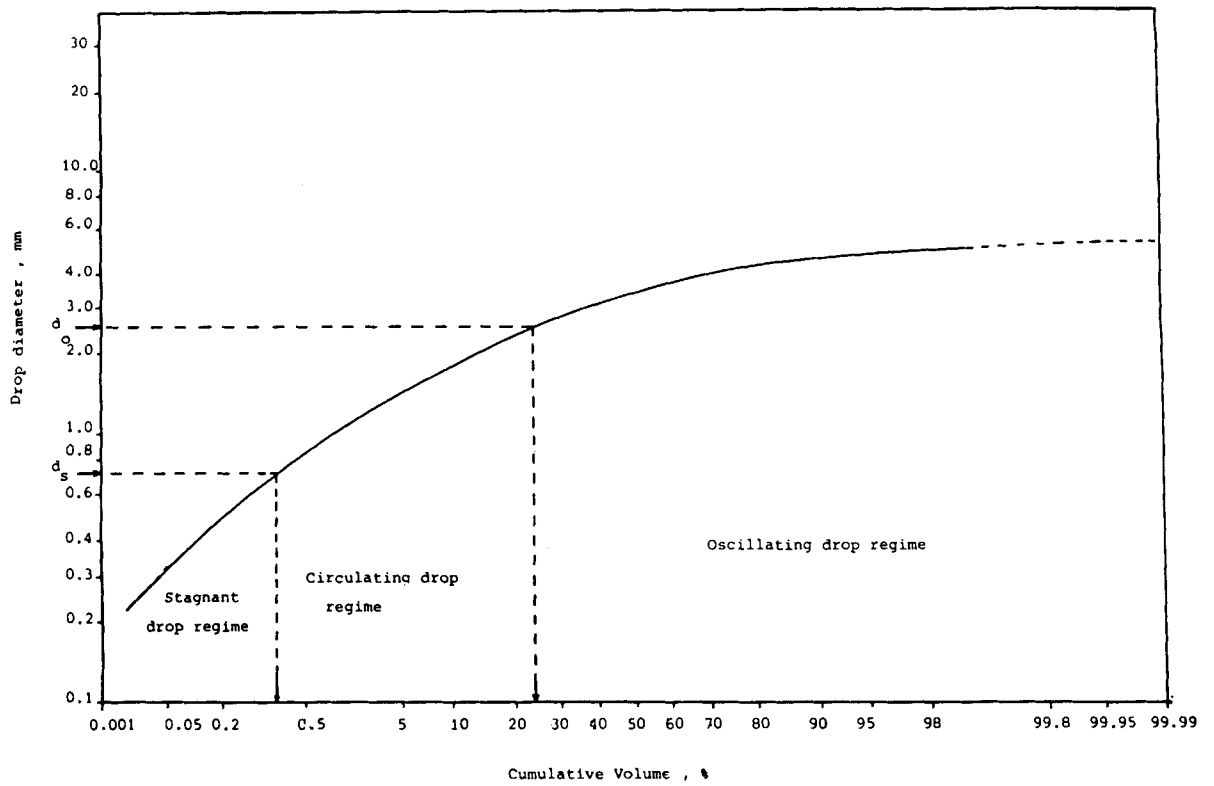

Figure 1. Typical drop size distribution.

in the circulating drops. Furthermore, the very small stagnant drops will approach saturation and will not play a large part in the mass transfer process. Hence it can be shown that the ratio of the rates of mass transfer to or from the circulating drops to that of the oscillating drops is,

$$\frac{N_{Ac}}{N_{Ao}} \simeq \left[\frac{x'}{5}\right]\left[\frac{p_c}{p_o}\right]\left[\frac{\Delta C_{mc}}{\Delta C_{mo}}\right] \text{ or } \left[\frac{N_{Ac}/(\Delta C)_{mc}}{N_{Ao}/(\Delta C)_{mo}}\right] \propto \frac{p_c}{p_o}$$

Since it is not possible to estimate the ratio of the driving forces it was considered preferable to base the fractional mass transfer coefficients on the volume fractions of the different drops in each regime.

The above procedure for estimating the overall mass transfer coefficient was assessed by comparing calculated composite overall mass transfer coefficients with those obtained experimentally from a study of the performance of a rotating disc extractor of diameter 0.45 m and height 4.3 m. Details of the equipment, experimental procedures and the results obtained are presented in the following sections.

EXPERIMENTAL ROTATING DISC CONTACTOR

A pilot-scale rotating disc contactor (RDC) was designed and constructed with fourteen compartments as illustrated in Figure 2. The principal dimensions of the column were:

Column internal diameter	0.45 m
Column effective height	4.3 m
Disc diameter	2.25×10^{-1} m
Compartment height	2.25×10^{-1} m
Stator opening	2.375×10^{-1} m

The column was assembled from two industrial glass pipe sections; the column internals and end flanges were constructed from stainless steel. The rotating disc was driven by a 0.2 kW motor and its speed was controlled by a gear box over the range 0–800 rpm. The speed of rotation was measured by an electronic tachometer in association with a photoelectric probe focused onto a vertical slot on the rotor shaft near the top of the column. Four, 2.0 m^3 stainless steel tanks were installed as receivers for the feed, solvent, extract, and raffinate and the flowrates of each stream to and from the column were measured by rotameters as shown on the flow diagram in Figure 2. Nine sample points were provided: one each at the dispersed phase inlet and continuous phase outlet, and seven along the length of the column above the distributor, and in compartments 3, 6, 9 and 12, and at the exit below the interface. Each column sample point was formed by drilling a 1.0×10^{-2} m hole into the glass wall of the column and then inserting a 0.6×10^{-2} m diameter tube containing a quick-acting toggle valve. The sample tube arrangement was sealed against leaks by a polytetrafluoroethylene gland.

The equipment was located in a flameproof laboratory in which the atmosphere was exchanged 30 times per hour. The entering air temperature was controlled to 18.5–20°C and therefore no provision was made to control the temperature of the fluids processed, although the temperature of each stream was measured frequently during the course of an experiment.

EXPERIMENTAL PROCEDURE

The system acetone, Clairsol 350, and water was employed throughout this study. The Clairsol 350 solutions were always the dispersed phase; the aqueous phase constituted the continuous phase. Acetone was transferred both to and from the Clairsol 350 in separate experiments so that the effects of the direction of mass transfer could be investigated. Clairsol 350 is a parafinic hydrocarbon, principally decane, with a distillation range of 205 to 230°C; its principal phyical properties are: density, 783 kg/m^3; kinematic viscosity, 2.0×10^{-6} m^2/s; interfacial tension, 39.2×10^{-3} J/m^2.

The water used in the experimental work was deionized tap water and all solutions containing acetone were limited to 5.0% w/w in order to prevent the formation of emulsions. The phase equilibria of the system acetone-Clairsol 350-water was ascertained experimentally and the distributions of acetone between the other solvents at the experimental temperature are presented in Figure 3 (Al-Aswad, 1982).

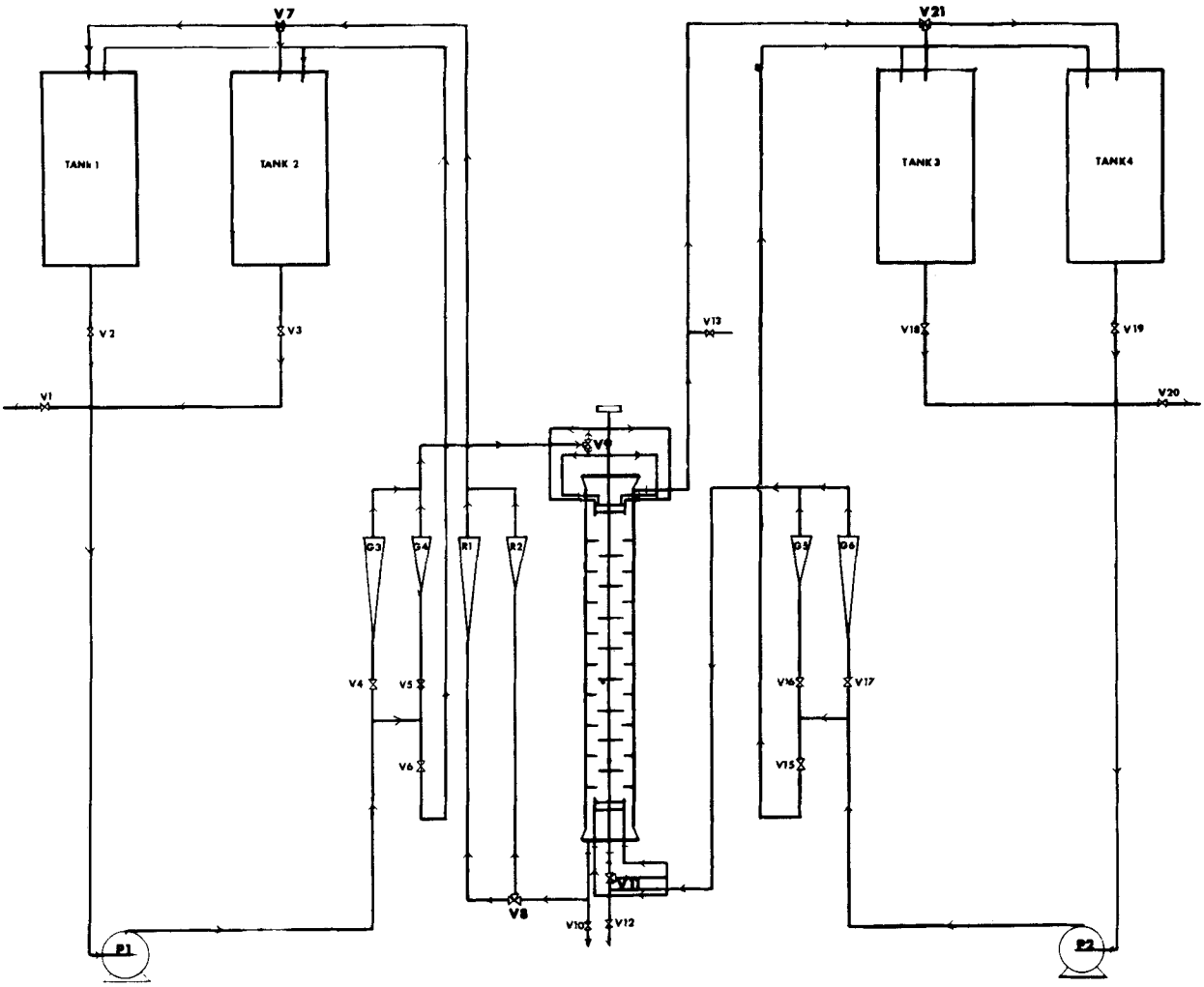

Figure 2. Flow diagram of RDC extraction equipment.

In all experiments the column was filled with the aqueous phase, then the rotor was started and its speed adjusted to that desired for the experiment. Next, the dispersed phase flow was introduced and the flowrate set to that desired for the experiment. When an interface had been established at the top of the column, the continuous phase flowrate was established and the extract and raffinate flows were adjusted to maintain a steady interface at the top of the column. Samples of feed, final extract, and raffinate were taken after the column had been operating for about 15 minutes and then again after a further 15 minutes to ascertain whether steady state mass transfer conditions had been established; generally, steady state had been established. 20-mL samples were then taken from each sample point, the phases separated immediately, and the acetone content of each phase determined by estimation for the absorbance in an ultraviolet spectrophotometer. The feed, solvent, extract, and raffinate flowrates were recorded and photographs of the dispersion emerging from the distributor and passing through compartments 2, 4, 6, 10, and 14 were taken for holdup and drop size measurements. Following this, all the valves of the column were rapidly closed and the rotor speed carefully reduced to encourage the dispersed phase to settle to the top of the column. When all the drops had been displaced from beneath the rotors and stators and coalesced into a band at the top of the column, the volume accumulated was measured to estimate the dispersed phase holdup. This holdup was compared with estimates obtained from the photographs taken of the dispersion in each of the compartments.

The flooding and "non-mass transfer" flow characteristics of the equipment used in this investigation have been reported elsewhere (Jeffreys, 1981; Al-Aswad, 1982) and therefore all the experiments undertaken in this study were restricted to a maximum 70% of the flooding flowrates reported above. Prints of the photographs taken were enlarged and the drop size and size distribution estimated using a Carl Zeiss Particle Analyzer.

A typical drop size distribution is presented in Figure 4, in which the drop size is plotted vs. the cumulative drop volume at two rotor speeds, 200 and 300 rpm. The values of d_{10}, d_{50}, and d_{90} were abstracted from this plot and the upper limit distribution parameters d_m; a' and δ calculated by applying the equations proposed by Mugele and Evans (1951). These parameters were then used to predict the upper limit distribution and the Sauter mean drop diameter d'_{32}; the results obtained are compared in Figure 5 with those found experimentally. Mugele and Evans estimations of d'_{32} were compared with those calculated from the experimental results; the mean deviation was found to be 5.2% at 200 rpm and 3.65 at 300 rpm. The values of d_{32} obtained in each experiment by the above procedure are given in Table 3.

Throughout this study an experiment was started by mutually saturating the phases and circulating each phase in a closed loop for about five hours, after which they were transferred to their respective tanks to settle overnight. The feed solution was then made up to the acetone concentration required for the experiment, normally in the range 1.5 to 5% w/w. The acetone concentration of the solvent was zero when it was aqueous and 0.5 w/w when Clairsol 350. Rotor speeds ranging from zero to 400 rpm were employed and the results obtained are presented in Tables 2 and 3.

DISCUSSION OF RESULTS

The overall experimental mass transfer coefficient for each experiment was calculated from the equation

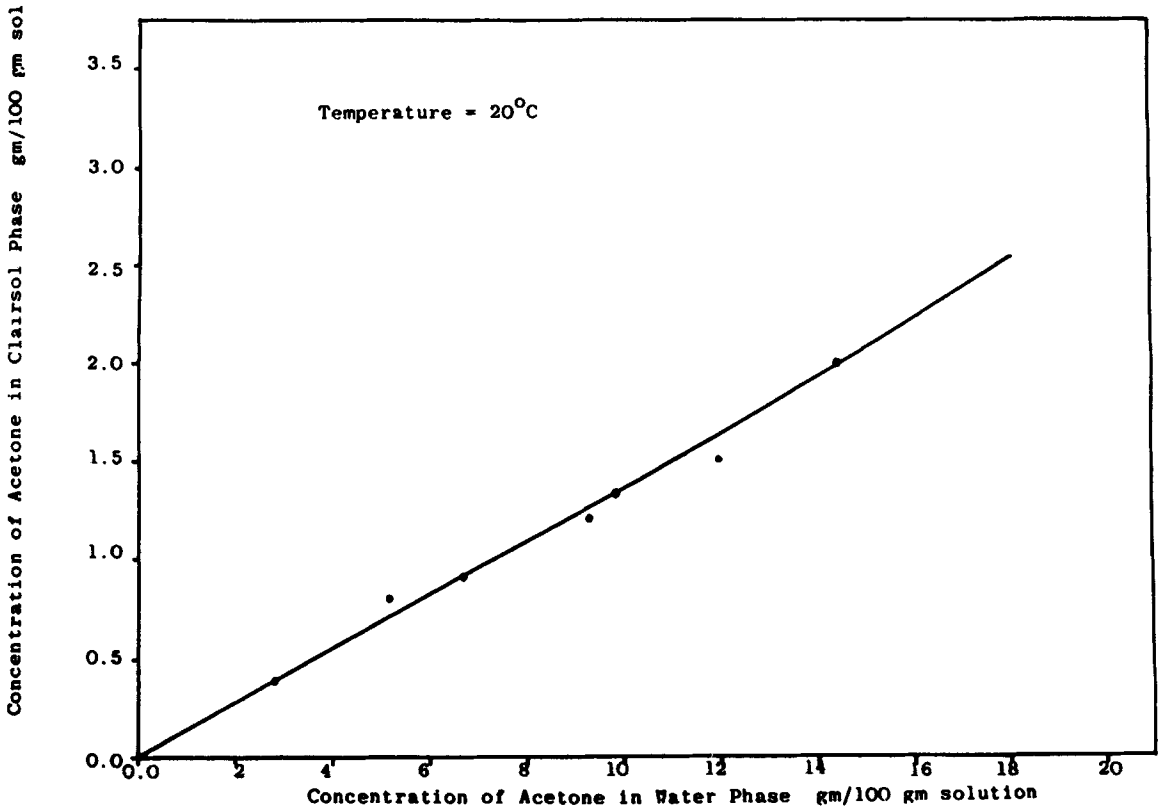

Figure 3. Equilibrium diagram for Clairsol-acetone-water system.

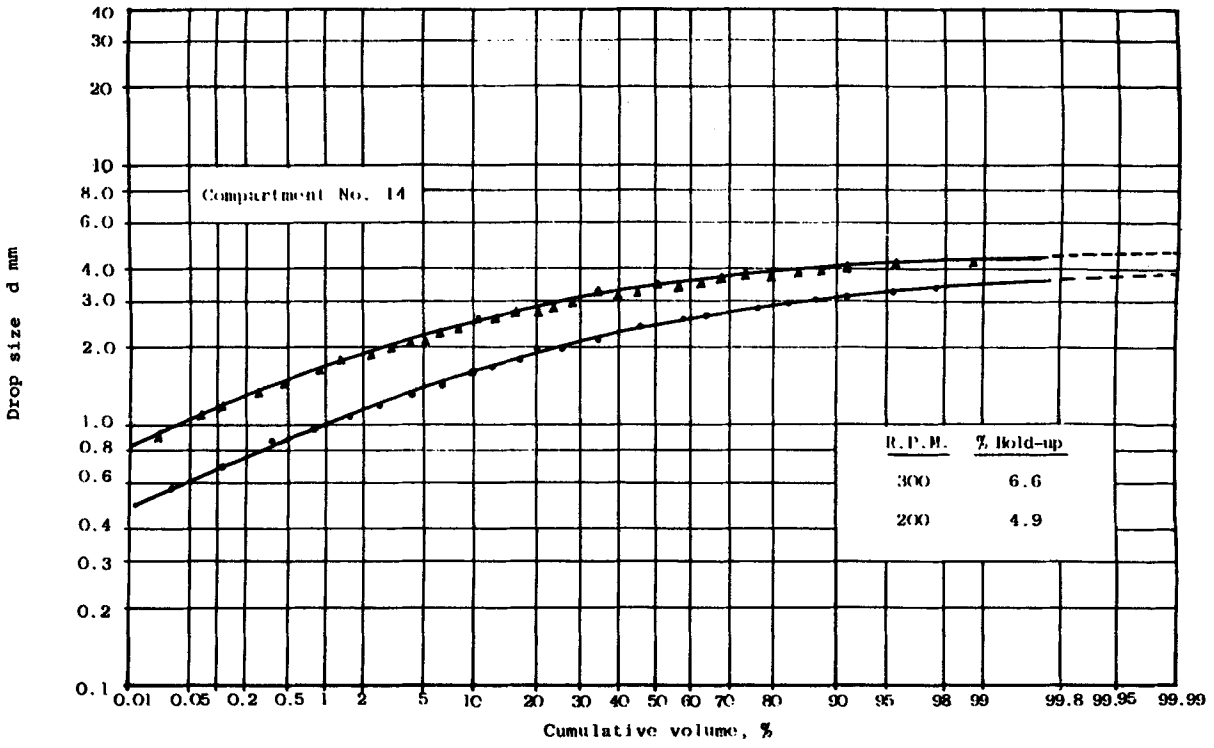

Figure 4. Typical drop size distributions at rotor speeds of 200 and 300 rpm.

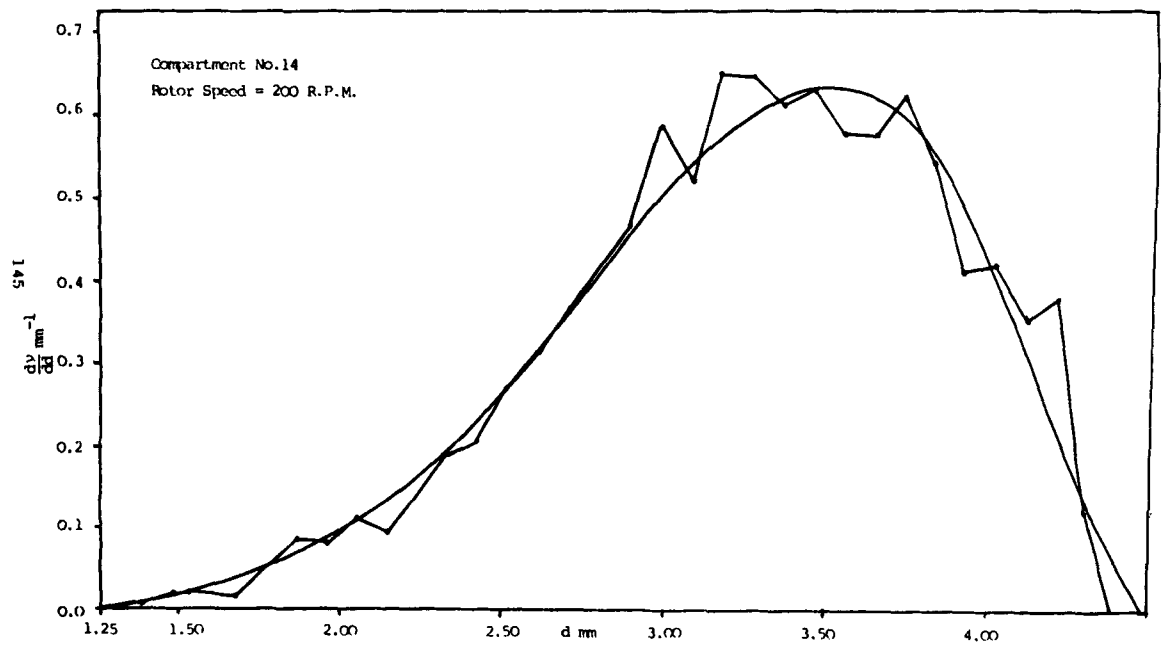

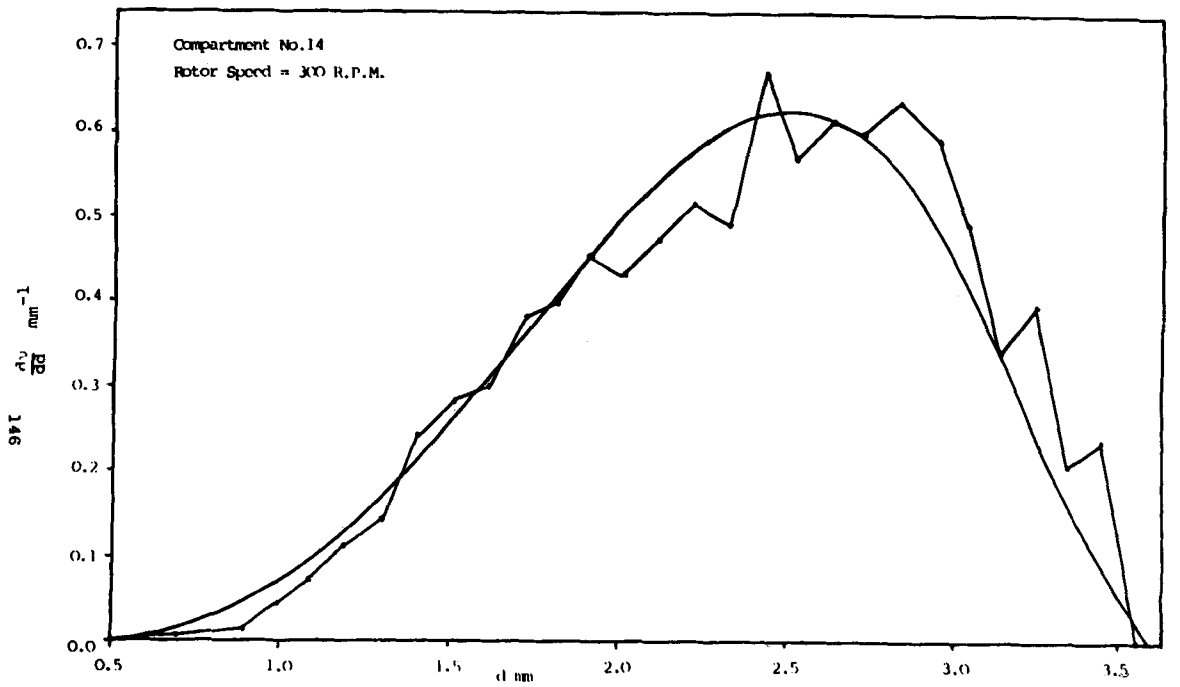

Figure 5. Comparison of experimental drop size distribution with upper limit distribution function.

$$N_A = KA(\Delta C)_m \tag{9}$$

where

N_A = the rate of mass transfer over the entire column,

A = the total interfacial area estimated from the calculated from the overall mass balance using the concentrations reported in Tables 2 and 3.

TABLE 2. MASS TRANSFER RESULTS

Run No.	Direction of Transfer*	N rpm	V_c cm/s	V_d cm/s	x_{in}	x_{out}	y_{in}	y_{out}
1	D → C	150	0.66	0.28	1.45	0.34	0.00	0.37
2	D → C	200	0.66	0.28	1.45	0.22	0.00	0.41
3	D → C	250	0.66	0.28	1.45	0.19	0.00	0.42
4	D → C	300	0.66	0.28	1.45	0.19	0.00	0.42
5	D → C	0.0	0.66	0.28	2.20	0.82	0.00	0.46
6	D → C	150	0.66	0.28	2.20	0.41	0.00	0.60
7	D → C	200	0.66	0.28	2.20	0.33	0.00	0.62
8	D → C	300	0.66	0.28	2.20	0.27	0.00	0.64
9	D → C	150	0.31	0.24	3.03	1.24	0.00	1.09
10	D → C	200	0.31	0.24	3.03	1.14	0.00	1.15
11	D → C	250	0.31	0.24	3.03	1.06	0.00	1.20
12	D → C	300	0.31	0.24	3.03	0.98	0.00	1.25
13	D → C	100	0.31	0.28	3.96	1.58	0.00	1.70
14	D → C	200	0.31	0.28	3.96	1.34	0.00	1.87
15	D → C	300	0.31	0.28	3.96	1.18	0.00	1.98
16	D → C	350	0.31	0.28	3.96	1.09	0.00	2.05
17	D → C	100	0.31	0.28	4.91	2.28	0.00	1.88
18	D → C	150	0.31	0.28	4.91	2.12	0.00	1.99
19	D → C	200	0.31	0.28	4.91	1.81	0.00	2.21
20	D → C	300	0.31	0.28	4.91	1.48	0.00	2.45
21	D ← C	100	0.31	0.24	0.45	1.10	5.52	5.12
22	D ← C	150	0.31	0.24	0.45	1.22	5.52	5.05
23	D ← C	200	0.31	0.24	0.45	1.28	5.52	5.01
24	D ← C	300	0.31	0.24	0.45	1.32	5.52	4.98

* D, dispersed phase, C, continuous phase.

TABLE 3. MASS TRANSFER RESULTS

Run No.	N g/s	Holdup %	Eff. Column Height cm	d_{32} cm	Total Interfacial Area A cm^2	ΔCm g/cm^3	K_{exp} cm/s
1	3.84	3.98	367	0.46	303,010.1	0.064	1.96×10^{-4}
2	4.25	4.52	371	0.35	457,204.1	0.054	1.72×10^{-4}
3	4.35	5.02	367	0.31	567,118.6	0.053	1.45×10^{-4}
4	4.35	5.76	369	0.24	845,090.9	0.053	9.71×10^{-5}
5	4.76	0.90	373	0.54	59,323.0	0.113	7.10×10^{-4}
6	6.21	3.95	363	0.49	279,237.3	0.102	2.18×10^{-4}
7	6.46	4.68	361	0.36	447,833.3	0.079	1.83×10^{-4}
8	6.67	6.03	363	0.26	803,371.5	0.071	1.17×10^{-4}
9	5.31	3.16	356	0.51	21,049.6	0.166	1.52×10^{-4}
10	5.61	3.78	358	0.37	349,010.8	0.157	1.02×10^{-4}
11	5.85	4.29	360	0.32	460,548.8	0.152	8.36×10^{-5}
12	6.08	5.51	378	0.24	828,128.9	0.148	4.96×10^{-5}
13	8.27	2.82	359	0.51	182,277.7	0.221	2.05×10^{-4}
14	9.10	3.70	357	0.39	323,199.8	0.184	1.53×10^{-4}
15	9.65	4.74	371	0.26	645,423.4	0.177	8.45×10^{-5}
16	9.97	6.62	373	0.21	1,122,052.9	0.167	5.32×10^{-5}
17	9.13	2.61	356	0.54	164,196.0	0.283	1.96×10^{-4}
18	9.69	2.82	358	0.52	185,265.5	0.258	2.03×10^{-4}
19	10.77	3.34	355	0.44	257,150.8	0.241	1.74×10^{-4}
20	11.91	4.10	360	0.32	434,038.3	0.226	1.21×10^{-4}
21	1.94	3.08	385	0.310	356,012.2	0.0124	4.29×10^{-4}
22	2.28	4.39	377	0.304	519,505.2	0.0185	2.37×10^{-4}
23	2.48	5.53	362	0.288	663,282.9	0.0207	1.81×10^{-4}
24	2.60	6.24	355	0.252	838,822.4	0.0211	1.47×10^{-4}

TABLE 4. COMPARISON OF EXPERIMENTAL AND CALCULATED THEORETICAL MASS TRANSFER COEFFICIENTS AT DIFFERENT ROTOR SPEEDS

Run No.	Direction of Transfer	Rotor Speed rpm	N g/sec	K_{exp} m/s	$K_{cal}^{(1)\dagger}$ m/s	$K_{cal}^{(2)\dagger}$ m/s
1	D → C	150	3.84	1.96×10^{-4}	2.47×10^{-4}	5.65×10^{-4}
2	D → C	200	4.25	1.72×10^{-4}	1.63×10^{-4}	4.16×10^{-4}
3	D → C	250	4.35	1.45×10^{-4}	1.31×10^{-4}	4.48×10^{-4}
4	D → C	300	4.35	9.17×10^{-5}	5.47×10^{-5}	1.73×10^{-4}
5	D → C	0.0	4.76	7.10×10^{-4}	6.58×10^{-4}	4.46×10^{-4}
6	D → C	150	6.21	2.18×10^{-4}	2.47×10^{-4}	5.39×10^{-4}
7	D → C	200	6.46	1.83×10^{-4}	1.60×10^{-4}	4.84×10^{-4}
8	D → C	300	6.67	1.17×10^{-4}	4.36×10^{-5}	1.42×10^{-4}
9	D → C	150	5.31	1.52×10^{-4}	2.49×10^{-4}	5.21×10^{-4}
10	D → C	200	5.61	1.02×10^{-4}	1.80×10^{-4}	5.07×10^{-4}
11	D → C	250	5.85	8.36×10^{-5}	8.59×10^{-5}	2.86×10^{-4}
12	D → C	300	6.08	4.96×10^{-5}	2.40×10^{-5}	7.34×10^{-4}
13	D → C	100	8.27	2.05×10^{-4}	3.09×10^{-4}	4.98×10^{-4}
14	D → C	200	9.10	1.53×10^{-4}	2.50×10^{-4}	6.39×10^{-4}
15	D → C	300	9.65	8.45×10^{-5}	5.96×10^{-4}	1.64×10^{-4}
16	D → C	350	9.97	5.32×10^{-5}	2.01×10^{-4}	5.50×10^{-4}
17	D → C	100	9.13	1.96×10^{-4}	3.25×10^{-5}	4.91×10^{-4}
18	D → C	150	9.69	2.03×10^{-4}	3.08×10^{-4}	5.01×10^{-4}
19	D → C	200	10.77	1.74×10^{-4}	2.69×10^{-4}	6.09×10^{-4}
20	D → C	300	11.91	1.21×10^{-4}	1.23×10^{-4}	3.85×10^{-4}
21	D ← C	100	1.94	4.29×10^{-4}	2.36×10^{-4}	6.10×10^{-4}
22	D ← C	150	2.28	2.37×10^{-4}	9.26×10^{-5}	3.14×10^{-4}
23	D ← C	200	2.48	1.81×10^{-4}	7.58×10^{-6}	7.58×10^{-6}
24	D ← C	300	2.60	1.47×10^{-4}	8.59×10^{-6}	8.59×10^{-6}

* D, Dispersed phase; C, continuous phase.
† $K_{cal}^{(1)}$ based on Rose & Kintner; $K_{cal}^{(2)}$ based on Angelo & Lightfoot.

relation [$a = (6h/d_{32})$]; where a is the specific interfacial area per unit volume of column and

V = the total volume of the column. Then:

$$A = aV \tag{10}$$

ΔC = the mean driving force which, because of the curvature in the operating line, was estimated by applying Simpson's rule thus:

$$(\Delta C)_m = \frac{\rho}{18}[\Delta y_{in} + 4\Delta y_1 + 2\Delta y_3 + 4\Delta y_6 + 2\Delta y_9 + 2\Delta y_{12} + \Delta y_{out}] \tag{11}$$

In all experiments in this study the flowrates and rotor speeds were such that drop sizes of between 0.01×10^{-3} m and 0.02×10^{-3} m would have to exist in the population for the drop Reynolds numbers to be less than 10. The fraction of drop sizes in this regime was negligible and therefore it was believed that the various dispersions consisted of circulating and oscillating drops only. The volume percentage of circulating drops p_c was estimated from the drop distribution diagram for the experiment. The appropriate mass transfer coefficients for the dispersed and continuous phases were calculated from Eqs. 3 and 4 in Table 1 and the overall coefficient $K_{o.c}$ evaluated from the normal series resistance equation. The remainder of the drops in the population were considered to be in the oscillating regime, that is [$p_o = (1 - p_c)$]. The mass transfer coefficients of the dispersed and continuous phases appropriate to this regime were calculated using Eqs. 5 or 6 with Eq. 7, and thereafter the overall coefficient $K_{o.o}$ was evaluated in the usual way. The calculated overall coefficient for the entire drop population K_{cal} was then obtained

$$K_{cal} = K_{o.c}p_c + K_{o.o}(1 - p_c) \tag{12}$$

Two values of K_{cal} were obtained from Eq. 12 depending on whether Eq. 5, due to Rose and Kintner (1966), or Eq. 6, due to Angelo and Lightfoot (1966), was applied to estimate the oscillating dispersed phase mass transfer coefficient. These values are reported in Table 4 together with the experimental overall mass transfer coefficient for each experiment.

In all experiments the experimental overall mass transfer coefficients agreed, to an order of magnitude, with those calculated by either of the above procedures, provided that the mean driving force was calculated by applying Simpson's rule as described by Eq. 11. When the log mean driving force was utilized the experimental coefficient was many orders of magnitude greater than the calculated values. This would be expected since application of Simpson's rule to the numerous point concentration driving forces along the length of the column attempts to correct for the curvature in the concentration profiles resulting from the variation in flowrate along the column and also from backmixing effects.

Examination of Table 4 shows that generally the rate of mass transfer increases with increasing rotor speed, but the overall mass transfer coefficient tends to decrease. This would be expected since the larger drops would tend to break up with increase in rotor speed, thereby decreasing the proportion of oscillating drops in the population. The advantages of a higher energy input relate to the increase in the interfacial area, through the higher holdup of the smaller drops, which increases more rapidly than the mass transfer coefficient decreases. Consequently the value of the overall volumetric mass transfer coefficient illustrates more clearly the effect of rotor speed, as shown in Figure 6. These results suggest that when

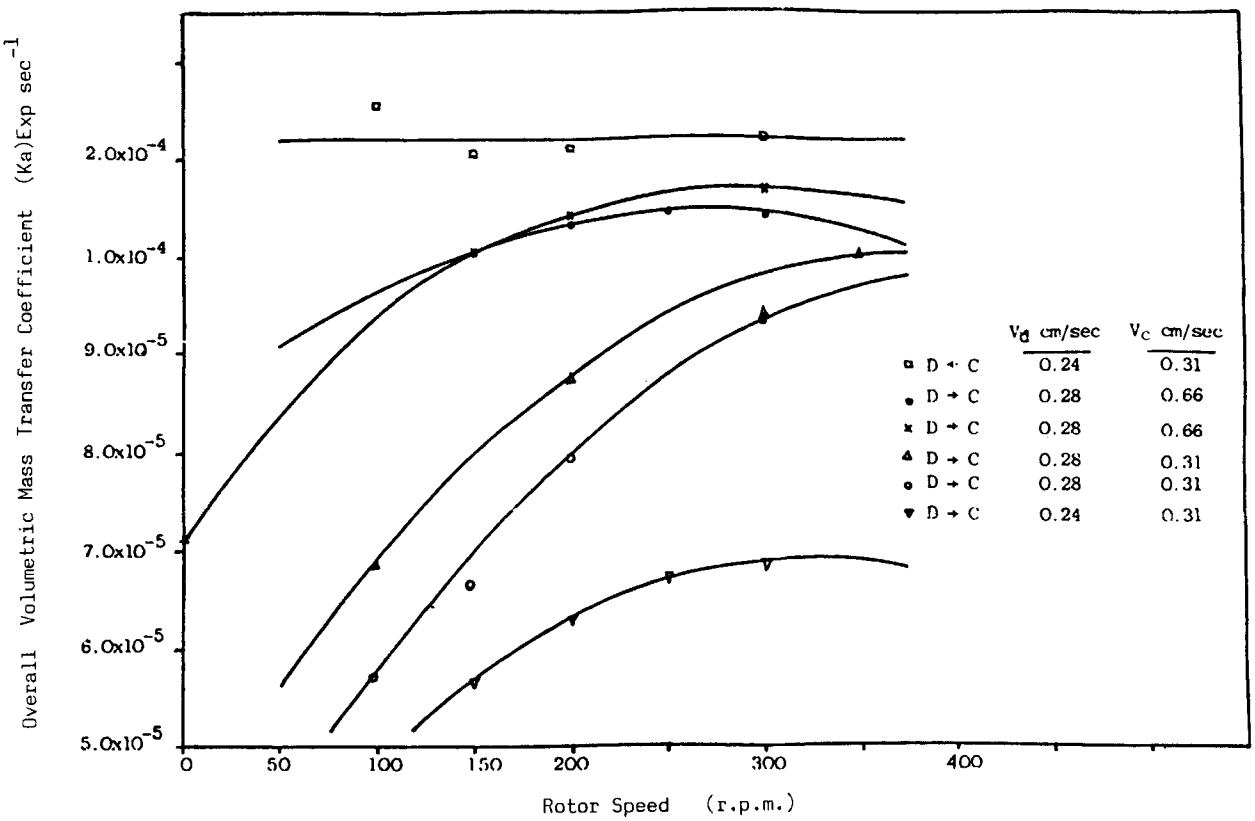

Figure 6. Effect of rotor speed on overall volumetric mass transfer coefficient.

TABLE 5. COMPARISON OF RATIOS OF EXPERIMENTAL TO CALCULATED THEORETICAL MASS TRANSFER COEFFICIENTS

Run No.	1 Direction of Transfer*	2 $\frac{K_{exp}}{K_{cal}^{(1)\dagger}}$	3 $\frac{K_{exp}}{K_{cal}^{(2)\dagger}}$	4 $\frac{K_{exp}}{K_{o.c}}$	5 $\frac{K_{exp}}{K_{o.o}^{(1)\dagger}}$	6 $\frac{K_{exp}}{K_{o.o}^{(2)\dagger}}$
1	D → C	0.79	0.35	23.93	0.79	0.35
2	D → C	1.05	0.35	15.64	0.75	0.25
3	D → C	1.11	0.32	14.80	0.68	0.20
4	D → C	1.78	0.56	10.18	0.51	0.15
5	D → C	1.08	1.59	18.68	1.08	1.60
6	D → C	0.88	0.40	25.95	0.88	0.40
7	D → C	1.14	0.38	16.64	0.82	0.27
8	D → C	2.68	0.82	13.42	0.64	0.17
9	D → C	0.61	0.29	17.88	0.61	0.29
10	D → C	0.57	0.20	11.47	0.46	0.16
11	D → C	0.97	0.29	9.09	0.42	0.12
12	D → C	2.07	0.68	5.66	0.31	0.08
13	D → C	0.67	0.41	18.30	0.67	0.41
14	D → C	0.61	0.24	14.71	0.60	0.23
15	D → C	1.42	0.52	9.19	0.40	0.13
16	D → C	2.65	0.97	5.46	0.34	0.08
17	D → C	0.60	15.93	15.93	0.60	0.40
18	D → C	0.66	18.62	18.62	0.66	0.40
19	D → C	0.65	17.86	17.86	0.63	0.28
20	D → C	0.98	13.57	13.57	0.51	0.16
21	D ← C	1.82	35.16	35.16	1.63	0.63
22	D ← C	2.56	29.70	29.70	1.21	0.34
23	D ← C	23.88	23.88	23.88	—	—
24	D ← C	17.11	17.11	17.11	—	—

* D, dispersed phase; C, continuous phase.
† $K_{cal}^{(1)}$, $K_{o.o}^{(1)}$ base on Rose & Kintner; $K_{cal}^{(2)}$, $K_{o.o}^{(2)}$ based on Angelo & Lightfoot.

the direction of mass transfer is from the dispersed phase to the continuous phase the overall volumetric coefficient increases rapidly with rotor speed, but is affected greatly by the total throughput of both phases. This is mainly an interfacial (i.e., holdup) effect.

Comparison of the experimental overall mass transfer coefficients with the calculated coefficients, using either the Rose-Kintner correlation or the Angelo-Lightfoot correlation for the oscillating drop dispersed phase mass transfer coefficient, shows that for the direction of mass transfer dispersed phase to continuous phase, the Rose-Kintner correlation gives better agreement. This is emphasized in Table 5 where the ratio of the experimental coefficient to each of the calculated values is presented. Column 2 gives the rates based on the Rose-Kintner correlation and there it is seen that the majority of the results are in the neighborhood of 1.0, whereas those in column 3, based on the Angelo-Lightfoot correlation, fluctuate considerably. The ratios given in column 4 are based on the assumption that no oscillating drops exist in the population, while columns 5 and 6 give ratios on the basis that all the drops oscillated. The calculated values inserted into column 5 were based on the Rose-Kintner correlation and those in column 6 on the Angelo-Lightfoot correlation. These ratios were evaluated to assess the extent of the oscillations induced through droplet collisions and additional turbulence generated by the flow of swarms of drops through the agitated continuous phase. The ratios in column 4 greatly exceed unity, confirming that a large proportion of the drops in the dispersion oscillate, whereas the ratios presented in columns 5 and 6 are less than 1.0, implying that not all the drops oscillate. However, when drops with Reynolds numbers less than 200 are induced to oscillate through collision with another drop, or through resonance by an oscillating drop in close proximity in the turbulent regime, it appears that these oscillations will be rapidly damped out when the dispersion passes out of the zones of high shear close to the rotor in the RDC. It is difficult to quantify the effects of these induced oscillations on the rate of mass transfer, but it appears that they are not large at the speeds of rotation of the discs in an RDC under normal operating conditions.

Finally, examination of the results for the direction of mass transfer continuous phase to dispersed phase generally confirms the comments made above, although the agreement between the experimental and calculated coefficients is poor. Most probably this is due to the very low rates of mass transfer encountered in these experiments, where small errors in the estimation of the concentrations would have an enormous effect on the mass transfer rate and coefficients. Attention must be drawn to the fact that the utilization of high concentrations of acetone in the continuous phase in such large equipment was prohibitively dangerous and expensive. Nevertheless the limited results obtained are generally supportive of those obtained when the direction of mass transfer was in the direction of dispersed phase to continuous.

NOTATION

A = total interfacial area, cm^2
a = interfacial area per unit of column volume, cm^2/cm^3
ΔC_m = actual mean concentration driving force, g/cm^3
D = molecular diffusivity, cm^2/s
d = drop diameter, cm
d_{32} = Sauter mean drop diameter, cm
h = dispersed phase holdup
K = overall mass transfer coefficient, cm/s
Ka = overall volumetric mass transfer coefficient, 1/s
K_{cal} = overall theoretical mass transfer coefficient, cm/s
K_{exp} = overall experimental mass transfer coefficient, cm/s
k_c = continuous phase mass transfer coefficient, cm/s
k_d = dispersed phase mass transfer coefficient, cm/s
m = equilibrium distribution coefficient
N = rate of mass transfer, g/s
n = number of drops
p = fraction of drops in dispersion undergoing circulation
Re = droplet Reynolds number, $dV_o\rho/\mu$
Sc = Schmidt number $\mu/\rho D$
Sh = Sherwood number kd/D
V = volume of column, cm^3
V = phase superficial velocity, cm/s
V_o = vertical relative velocity of drops, cm/s
x = solute concentration in the raffinate phase, g/g sol
x' = ratio d_{mo}/d_{mc}
y = solute concentration in the extract phase, g/g sol
y^* = equilibrium solute concentration in the extract phase, g/g sol

Greek Letters

ρ = density, g/cm^3
μ = viscosity, g/cm s
ω = frequency of oscillation, 1/s
ϵ = amplitude of oscillation
ϵ_o = function of amplitude of oscillation defined by Eq. 6

Subscripts

c = continuous phase or/and circulating drop
cal = calculated or theoretical
d = drop or/and dispersed phase
exp = experimental
m = mean
o = overall or/and oscillating drop
s = stagnant drop

LITERATURE CITED

Angelo, J. B., E. N. Lightfoot, and D. W. Howard, "Generalization of the Penetration Theory for Surface Stretch," *AIChE J.*, **12**, 751 (1966).

Al-Aswad, K.K.M. "Liquid Extraction in a Pilot-Scale Rotating Disc Contactor," Ph.D. Thesis, University of Aston in Birmingham, UK (1982).

Garner, F. H., A. Foord, and M. Tayeban, "Mass Transfer from Circulating Liquid Drops," *J. App. Chem.*, **9**, 315 (1959).

Garner, F. H., and M. Tayeban, "Continuous Phase Mass Transfer Coefficients in Oscillating Drops," *Anal. Real. Soc. Espan. Fis. Quim.* (*Madrid*), **B56**, 479 (1960).

Jeffreys, G. V., K.K.M. Al-Aswad, and C. J. Mumford, "Drop Size Distribution and Dispersed Phase Holdup in a Large Rotating Disc Extractor," *Sep. Sci. and Tech.*, **16**, 1217 (1981).

Kronig, R., and J. C. Brink, "Dispersed Phase Mass Transfer Coefficients," *Appl. Sci. Res.*, **A2**, 142, (1960).

Mugele, R. A., and H. D. Evans, "Drop Size Distribution in Sprays," *Ind. Eng. Chem.*, **43**, 1,317, (1951).

Olney, R. B., "Droplet Characteristics in a Countercurrent Contactor," *AIChE J.*, **10**, 827 (1964).

Rose, P. M., and R. C. Kintner, "Mass Transfer from Large Oscillating Drops," *AIChE J.*, **12**, 530 (1966).

Treybal, R. E., *Liquid Extraction*, 2nd Ed., McGraw-Hill, New York (1963).

Manuscript received June 4, 1984; revision received Oct. 10 and accepted Oct. 15, 1984.